

GEOMETRIC SIGNATURES OF COMPOSITIONALITY ACROSS A LANGUAGE MODEL’S LIFETIME

Jin Hwa Lee*

University College London
London, United Kingdom
jin.lee.22@ucl.ac.uk

Thomas Jiralerspong*

Université de Montréal
Montreal, Canada
thomas.jiralerspong@mila.quebec

Lei Yu

University of Toronto
Toronto, Canada
jadeleiyu@cs.toronto.edu

Yoshua Bengio

Université de Montréal
Montreal, Canada
yoshua.bengio@mila.quebec

Emily Cheng

Universitat Pompeu Fabra
Barcelona, Spain
emilyshana.cheng@upf.edu

ABSTRACT

Compositionality, the notion that the meaning of an expression is constructed from the meaning of its parts and syntactic rules, permits the infinite productivity of human language. For the first time, artificial language models (LMs) are able to match human performance in a number of compositional generalization tasks. However, much remains to be understood about the representational mechanisms underlying these abilities. We take a high-level geometric approach to this problem by relating the degree of compositionality in a dataset to the intrinsic dimensionality of its representations under an LM, a measure of feature complexity. We find not only that the degree of dataset compositionality is reflected in representations’ intrinsic dimensionality, but that the relationship between compositionality and geometric complexity arises due to learned linguistic features over training. Finally, our analyses reveal a striking contrast between linear and nonlinear dimensionality, showing that they respectively encode formal and semantic aspects of linguistic composition.

1 INTRODUCTION

By virtue of linguistic compositionality, few syntactic rules and a finite lexicon can generate an unbounded number of sentences (Chomsky, 1957). That is, language, though seemingly high-dimensional, can be explained using relatively few degrees of freedom. A great deal of effort has been made to test whether neural language models (LMs) exhibit human-like compositionality (Hupkes et al., 2019; Baroni, 2019; McCoy, 2022). We take a geometric view of this question, asking how an LM’s representational structure reflects and supports compositional understanding over training.

If a language model is a good model of language, we expect its internal representations to reflect the relatively few variables underlying the latter. That is, representations should reflect the *manifold hypothesis*, or the notion that real-life, high-dimensional data lie on a low-dimensional manifold (Goodfellow et al., 2016). The dimension of this manifold, or *intrinsic dimension* (ID), is then the minimal number of degrees of freedom required to describe it without suffering from information loss

*Equal Contribution

(Goodfellow et al., 2016; Campadelli et al., 2015). The manifold hypothesis has indeed been attested for linguistic representations: LMs have been found to compress inputs to an ID orders-of-magnitude lower than their extrinsic dimension (Cai et al., 2021; Cheng et al., 2023; Valeriani et al., 2023).

Compositionality permits the atoms of language to locally combine with others, creating global meaning (Frege, 1948; Chomsky, 1999). As such, a complex array of meanings at the level of a phrase is explained by simple rules of composition. A natural question is whether the inherent simplicity of linguistic utterances, enabled by compositionality, manifests in representation manifolds of low complexity, described by the manifolds’ intrinsic dimension. Thus far in the literature, an explicit link between degree of compositionality and representational ID has not been established. To bridge this gap, in a series of controlled experiments on causal language models and a custom dataset with tunable compositionality, we provide the first experimental insights into the relationship between the degree of compositionality of inputs and the ID of their representations over the course of training.

Using our controlled stimulus stimuli and the LMs’ training data, we reproduce the established finding that LMs represent linguistic inputs on low-dimensional, nonlinear manifolds. We also show for the first time that LMs expand representations into high-dimensional linear subspaces, concretely, that **(1)** nonlinear and linear representational dimension scale differently with model size. We show the relevance of geometry to function over LM training, in particular that **(2)** LMs’ representational geometry tracks a phase transition in their linguistic competence. Different from past work, we consider two different kinds of compositionality: compositionality of *form*, or superficial combinatorial complexity, and compositionality of *meaning*, or semantic complexity; as well as two measures of dimensionality, nonlinear and linear. We not only find that geometric feature complexity reflects input compositionality, but crucially that ***nonlinear ID encodes meaning compositionality while linear dimensionality encodes form compositionality***, in a way that arises over training: **(3)** nonlinear ID preserves the degree of input compositionality as an inductive bias of the model, but reflects the degree of semantic complexity at the end of training, and **(4)** linear dimensionality, not nonlinear ID, highly correlates to the superficial combinatorial complexity of inputs. Overall, results reveal a contrast between linear and nonlinear measures of feature complexity that suggests their relevance to form and meaning in how LMs process language.

2 BACKGROUND

Compositionality It has long been a topic of debate whether neural networks also exhibit human-like compositionality when processing natural language (Fodor & Pylyshyn, 1988; Smolensky, 1990; Marcus, 2003). This debate has fueled an extensive line of empirical exploration that assesses the compositionality of neural networks in language modeling via synthetic data (Bentivogli et al., 2016; Lake & Baroni, 2018; Bahdanau et al., 2018) and natural language stimuli (Sathe et al., 2023; Dankers et al., 2022; Press et al., 2023). After the recent introduction of large language models with human-level linguistic capabilities (Wei et al., 2022), researchers have shown via mechanistic interpretability analyses that LMs often extract individual word meanings in early layers, and compose them via later-layer attention heads to construct semantic representations for multi-word expressions (Haviv et al., 2023; Geva et al., 2023). We use complementary tools to understand compositionality: rather than neurons and circuits, we link compositionality to the geometric properties of a model’s embedding space which describe its learned feature complexity.

Language defines a mapping from form to meaning (de Saussure, 1916). *Form* is the physical shape of an utterance, for example, the sequence of letters or morphemes when written, or sounds when spoken. Broadly, *meaning* is the concepts or entities to which the forms refer. Unlike prior work, we make a distinction between form and meaning composition, where the formal composition relates to the combinatorial complexity of the data, and semantic composition relates to the ability to construct sentence-level meaning from word meaning. While, in grammatical sentences, meaning composition often inherits from form composition, we disentangle them by creating agrammatical versions of the dataset, further described in the Methods.

The manifold hypothesis and low-dimensional geometry Deep learning problems are often considered high-dimensional, but research suggests that they have low-dimensional intrinsic structure. In computer vision, studies have shown that common learning objectives and natural image data reside on low-dimensional manifolds (Li et al., 2018; Pope et al., 2021; Valeriani et al., 2023; Psenka et al.,

2024). Similarly, learning dynamics of neural LMs have been shown to occur within low-dimensional parameter subspaces (Aghajanyan et al., 2021; Zhang et al., 2023). The nonlinear, low-dimensional structure that emerges in the semantic space of these models, in contrast with models’ tendency to expand representations into high-dimensional linear subspaces (Jazayeri & Ostojic, 2021), has been found to reduce learning complexity (Cheng et al., 2023; Pope et al., 2021), and likely follows from the training objective of predicting sequential observations (Recanatani et al., 2021).

In the linguistic domain, the geometry of representations has been examined in various contexts. Recent work characterizes the organization of semantic concepts in representation space (Engels et al., 2024; Park et al., 2024; Balestrieri et al., 2024; Doimo et al., 2024); it has been found that representational geometry can explicitly encode sparse tree-like syntactic structures (Andreas, 2019; Murty et al.; Alleman et al., 2021); and that linguistic categories such as part-of-speech are represented in low dimensional linear subspaces (Mamou et al., 2020; Hernandez & Andreas, 2021). Most similar to our setup, Cheng et al. (2023) reported the intrinsic dimension of representations over layers as a measure of feature complexity for several natural language datasets, finding an empirical relationship between information-theoretic and geometric compression. However, our work is the first to explicitly relate the compositionality of inputs, a critical feature of language, to the number of degrees of freedom, or intrinsic dimension, of its representation manifold.

Language model training dynamics Most research on LMs focuses on the final configuration of the model at the end of pre-training. Yet, recent work shows that learning dynamics can elucidate the behavior and computational mechanisms of LMs (Chen et al., 2024; Singh et al., 2024; Tigges et al., 2024). It has been found that, over training, LMs’ weight matrices become higher-rank (Abbe et al., 2023), their representations higher dimensional (Cheng et al., 2024), and their gradients increasingly diffuse (Weber et al., 2024). Over finetuning, representational dimensionality has been found to change in concert with geometric properties like cluster reorganization (Doimo et al., 2024).

Phase transitions during LM training have been found for some, but not all, aspects of language learning. Negative evidence includes that LM circuits involved in linguistic subtasks are stable (Tigges et al., 2024) and gradually reinforced (Weber et al., 2024) over training. Positive evidence for learning phase transitions includes that the ID of BERT’s final [CLS] representation tracks sudden syntax acquisition and drops in training loss (Chen et al., 2024), with similar observations on Transformers trained on formal languages (Lubana et al., 2024). Our work supplements these results by investigating how the interaction between compositional understanding of language and geometric complexity of its representation arises over training.

3 SETUP

We consider the relationship between a dataset’s degree of compositionality and its representational complexity under an LM. Here, we describe the models, dataset generation, compositionality quantification, and feature complexity estimation.

3.1 MODELS

We evaluate Transformer-based *causal* language models from the Pythia family (Biderman et al., 2023), as Pythia is one of the only model suites to release intermediate training checkpoints. Models are trained on The Pile, a large natural language corpus encompassing encyclopedic text, books, social media, code, and reviews (Gao et al., 2020). Over training, models are tasked to predict the next token given context, subject to a negative log-likelihood loss. Experiments are performed on all models in sizes $\in \{14m, 70m, 160m, 410m, 1.4b, 6.9b, 12b\}$.

Pre-training analysis For the three intermediate sizes 410m, 1.4b, and 6.9b, we report model performance throughout the pre-training phase on the set of evaluation suites provided by (Biderman et al., 2023; Gao et al., 2024), further described in Appendix F. This encompasses a range of higher-level linguistic and reasoning tasks, spanning from long-range text comprehension (Paperno et al., 2016) to commonsense reasoning (Bisk et al., 2019). The evolution of task performance provides a cue for the type of linguistic knowledge learned by the model by a certain training checkpoint.

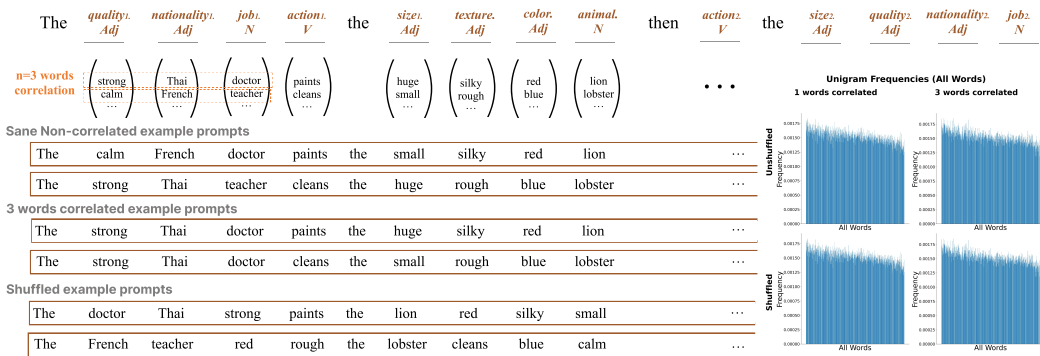


Figure 1: **Dataset structure and distributional properties.** **Top:** The structure of the stimulus dataset. The top row shows the ordering of word categories, such as quality.ADJ or animal.N; below it, the vocabulary for each category, including words like “strong” (quality.ADJ) and “lion” (animal.N), respectively. When controlling the degree of dataset compositionality, contiguous word positions are coupled. For instance, when $k = 3$, the first vocabulary indices for quality₁.ADJ, nationality₁.ADJ, and job₁.N are tied together, such that “strong Thai doctor” or “calm French teacher” can be sampled, but “strong French doctor” cannot. **Left:** Examples of generated prompts for the normal, $k = 3$, and shuffled settings. **Right:** When controlling the compositionality across $k = 1 \cdots 4$, word unigram frequencies are preserved in the resulting datasets, shown in the distributions looking identical.

3.2 DATASETS

As we consider the relationship between the degree of compositionality and geometric feature complexity, we create a custom grammar whose compositional structure we can control. In addition, we replicate experiments on The Pile in order to compare results to a general slice of natural language.

3.2.1 CONTROLLED GRAMMAR

Our stimulus dataset consists of grammatical nonce sentences from the grammar illustrated in Figure 1. To create the grammar, we set 12 semantic categories and randomly sample a vocabulary of 50 words for each category, where the categories’ vocabularies are disjoint. The categories include 5 adjective types (quality, nationality, size, color, texture), 2 noun types (job, animal) and 1 verb type. We use a simple, fixed syntactic structure by ordering the word categories:

The [quality₁.ADJ][nationality₁.ADJ][job₁.N] [action₁.V] the [size₁.ADJ][texture.ADJ] [color.ADJ][animal.N] then [action₂.V] the [size₂.ADJ][quality₂.ADJ][nationality₂.ADJ] [job₂.N].

This produces sentences that are 16 words long. The order is chosen so that the generated sentences are grammatical and that the adjective order complies with the accepted ordering for English (Dixon, 1976). Vocabularies are chosen such that the sentences are semantically coherent. For example, for the first verb, the agent is a person and patient is an animal, so the possible verbs are constrained to permit “walks”, but not “types”. The vocabularies for each category may be found in Appendix E.

Although the syntactic structure and individual vocabulary items are likely seen during training, words are sampled independently for each category without considering their probability in relationship to other words in the sentence. Therefore, generated sentences are highly unlikely to be in the training data.¹ Then, when encountering these sentences for the first time, a frozen LM must successfully construct their meanings from the meanings of their parts, or compositionally generalize.

¹We cannot verify that utterances aren’t in the training set, as at the time of submission, it is not possible to search The Pile.

Controlling compositionality We modify the grammar in order to vary the dataset’s degree of compositionality. While linguistic compositionality spans many interpretations (Hupkes et al., 2019),² we are interested in two specific types: (1) composition of *forms*, or *combinatorial complexity* of the dataset, where a dataset is more compositional if it contains more unique word combinations; (2) composition of *meanings*, or sentence-level *compositional semantics*, where sentence meaning is composed, via syntax, from word meanings.

First, to control for dataset combinatorial complexity, we couple the values of k contiguous word positions for $k = 1 \cdots 4$. That is, the sequence’s atomic units are sets of k adjacent words, or k -grams, sampled independently. This constrains the degrees of freedom in sampling to l/k where $l = 12$ is the number of categories: for instance, in the 1-coupled setting, each word is sampled independently, hence 12 degrees of freedom; in the 2-coupled setting, each bigram is sampled independently, hence 6 degrees of freedom. Varying k maintains the dataset’s unigram distribution by design (see Figure 1 right), but constrains the dataset’s k -gram distributions, or combinatorial complexity.

To investigate compositional semantics, we randomly shuffle the words in each sequence. This destroys syntactic coherence, and in turn, the overall meaning of the sentence. It instead preserves superficial distributional properties like word count and word co-occurrences at the sentence level, as well as unigram frequencies (see Figure 1 right). Then, LM behavior on grammatically sane vs. shuffled sequences proxies compositional vs. lexical-only semantics.

For each setting in $k \in \{1 \cdots 4\} \times \{\text{sane, shuffled}\}$, we sampled a dataset of $N = 50000$ sequences, then randomly split into 5 disjoint sets of 10000 sequences. Results are reported across data splits.

Measuring formal and semantic compositionality Form compositionality is controlled by the dataset combinatorial complexity. We quantify form compositionality of the controlled dataset by its Kolmogorov complexity, estimated using `gzip`,³ a popular lossless compression algorithm. We estimate the Kolmogorov complexity for $k \in \{1 \cdots 4\} \times \{\text{sane, shuffled}\}$ by the `gzip`-compressed dataset size in kilobytes, then correlate it to feature complexity measures (Section 3.3) for each layer.

Meaning complexity differs from form complexity. For example, the data $[\text{cat}, \text{lion}, \text{puma}]$ are related semantically but not formally. As there is no unified definition for semantic complexity (Pollard & Biermann, 2000; Chersoni et al., 2016), we do not attempt to quantify it. But, as sane sequences are grammatical and semantically coherent, it is guaranteed for sane datasets that meaning complexity is monotonic in form complexity. In addition, as shuffling removes sequence-level semantics, meaning complexity is guaranteed to be lower on shuffled compared to sane text, by definition.

3.2.2 THE PILE

Although we focus on the controlled grammar in order to vary compositionality, to ensure that results are not an artifact of our prompts, we replicate experiments on The Pile, a general slice of natural language consisting of encyclopedic text, social media, reviews, news articles, and books. We uniformly sample $N = 50000$ sequences in The Pile, each consisting of 16 words, the same length as sequences in the controlled grammar, and report results over 5 random data splits.

3.3 MEASURING FEATURE COMPLEXITY VIA DIMENSIONALITY ESTIMATION

We are interested in how the geometric complexity of representations reflects the inputs’ degree of compositionality. In particular, we consider representations in the Transformer’s *residual stream* (Elhage et al., 2021). Because sequence lengths may slightly vary due to the tokenization scheme, in line with prior work (Cheng et al., 2023; Doimo et al., 2024), we aggregate over the sequence by taking the last token representation, as, due to causal attention, it is the only to attend to the entire context.

For each layer and dataset, we compute both a nonlinear and a linear measure of dimensionality. Nonlinear and linear dimensionality have key conceptual differences. The nonlinear I_d is the number of degrees of freedom, or latent features, needed to describe the underlying manifold (Campadelli

²We do not consider the recursive, hierarchical nature of compositionality theorized by Chomskian linguists. We leave, e.g., different levels of syntactic embedding to future work.

³The true Kolmogorov complexity is theoretically intractable. We approximate it as others have, using `gzip` (Jiang et al., 2023).

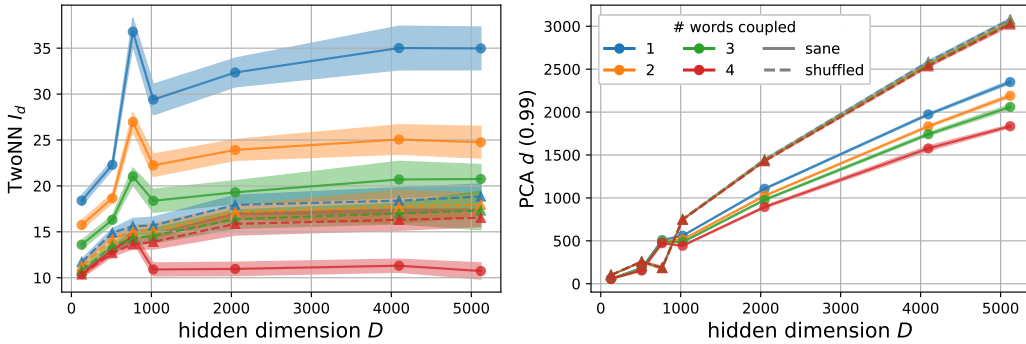


Figure 2: **Mean dimensionality over model size.** Mean nonlinear I_d (left) and linear d (right) over layers is shown for increasing LM hidden dimension. While nonlinear I_d does not depend on hidden dimension D (flat lines), PCA d scales linearly in D . Curves are averaged over 5 data splits, ± 1 SD.

et al., 2015; Facco et al., 2017), see Appendix D for discussion. This differs from the *linear* effective dimensionality d , the dimension of the minimal linear subspace that contains the set of representations. Throughout, we will use *dimensionality* to refer to both nonlinear and linear estimates. When appropriate, we will specify I_d as the nonlinear ID, d as the linear effective dimensionality, and D as the extrinsic dimensionality, or hidden dimension of the model. Since an I_d -dimensional manifold can be embedded in a $\geq I_d$ -dimensional linear subspace, we always have that $I_d \leq d \leq D$.

Intrinsic dimension We report the nonlinear I_d using the TwoNN estimator of Facco et al., 2017. We choose TwoNN as opposed to other measures of nonlinear dimensionality for several reasons. First, it is highly correlated to other state-of-the-art estimators, such as the Maximum Likelihood Estimator (MLE) of Levina & Bickel (2004), for both synthetic point cloud benchmarks (Facco et al., 2017) and LM representations (Cheng et al., 2023). Second, it relies on minimal assumptions of local uniformity up to the second nearest neighbor of a point, in contrast to other estimators that impose stricter assumptions, for instance, global uniformity (Albergante et al., 2019). Third, TwoNN and correlated estimators enjoy precedence in related manifold estimation literature (Cheng et al., 2023; Pope et al., 2021; Chen et al., 2024; Tulchinskii et al., 2023; Ansuini et al., 2019). In addition to TwoNN in the main text, we also test MLE in Appendix C, confirming they are highly correlated.

The TwoNN estimator works as follows. Points on the underlying manifold are assumed to follow a locally homogeneous Poisson point process. Here, local refers to the neighborhood about each point x encompassing x 's first and second nearest neighbors. Let $r_k^{(i)}$ be the Euclidean distance between x_i and its k th nearest neighbor. Then, under the mentioned assumptions, the distance ratios $\mu_i := r_2^{(i)}/r_1^{(i)} \in [1, \infty)$ follow the cumulative distribution function $F(\mu) = (1 - \mu^{-I_d})\mathbf{1}[\mu \geq 1]$. This yields an estimator for the ID, $I_d = -\log(1 - F(\mu))/\log \mu$. Finally, given representations $\{x_i^{(j)}\}_{i=1}^N$ for LM layer j , $I_d^{(j)}$ is numerically fit via maximum likelihood estimation over all datapoints.

Linear effective dimension To estimate the linear effective dimension d , we use Principal Component Analysis (PCA) (Jolliffe, 1986) with a variance cutoff of 99%. We compared to the Participation Ratio (PR) (Gao et al., 2017), a linear dimensionality measure often used in the computational neuroscience literature (cf. Chung et al. (2018); Recanatesi et al. (2019)), finding it to produce uninterpretable results, see Appendix C. For this reason, we focus on PCA in the main text.

4 RESULTS

We find that representational dimensionality reflects compositionality in ways that are predictable over pre-training and model scale. First, we show that language models represent linguistic data on low-dimensional, nonlinear manifolds, but in high-dimensional linear subspaces that scale linearly with the hidden dimension. Then, we show that, over training, geometric feature complexity is informative of an LM's linguistic competence, such that both exhibit a nontrivial phase transition

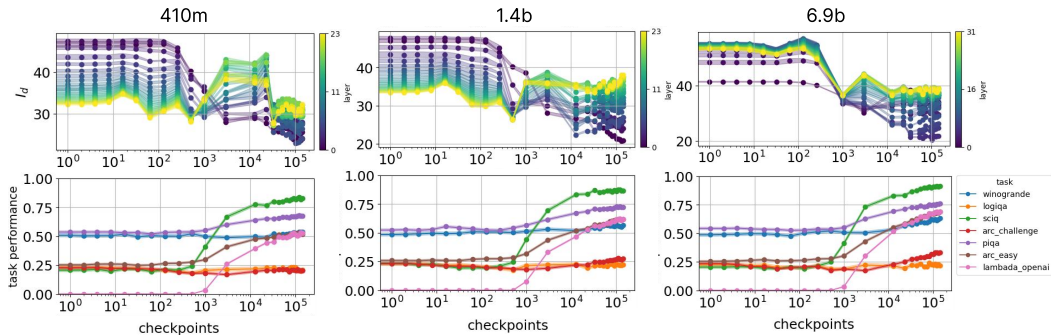


Figure 3: **ID tracks task performance.** **Top:** Layerwise I_d development of Pythia-410m, 1.4b, and 6.9b over pre-training. The phase transition of ID around checkpoint 10^3 is persistent across the model sizes. **Bottom:** Zero-shot task performance of various LM evaluation tasks of the same models across pre-training. Also around checkpoint 10^3 , linguistic competence measured by task performance starts to increase for all models.

that marks emergence of syntactic and semantic abilities. Finally, we show that representational dimensionality predictably reflects the degree of compositionality, both in terms of combinatorial complexity and sequence-level semantics and analyze its evolution over training. For brevity, we focus on model sizes 410m, 1.4b, and 6.9b in the main text, with full results in the appendix.

4.1 NONLINEAR AND LINEAR FEATURE COMPLEXITY SCALE DIFFERENTLY WITH MODEL SIZE

Like in previous work (Cai et al., 2021; Valeriani et al., 2023; Cheng et al., 2024), we confirm that input data are represented on a nonlinear manifold with orders-of-magnitude lower dimension than the embedding dimension. In particular, for both the controlled dataset, see Figure 2, and for The Pile, see Figure H.1, we find that $I_d \sim O(10)$ while linear $d, D \sim O(10^3)$.

Our novel finding is that nonlinear and linear dimensionality measures scale differently with model size. We fit linear regressions $D \sim \langle d \rangle_{\text{layer}}$ and $D \sim \langle I_d \rangle_{\text{layer}}$ for each setting in $k \in \{1 \cdots 4\} \times \{\text{sane, shuffled}\}$, as well as for The Pile. Linear effect sizes α , correlation coefficients R , and p-values for each setting are reported in Tables G.1 and H.1 (Pile), and the curves themselves found in Figures 2 and H.1 (Pile). For the controlled dataset, d scales *linearly* with hidden dimension D , shown in Figure 2 (right); all cases show a highly significant linear fit with $R > 0.99$ and $p < 0.005$ (Table G.1). Meanwhile, I_d stabilizes to a low range $\sim O(10)$ regardless of D , see Figure 2 (left): here, in all cases, the effect sizes $\alpha \approx 0$ and fits are not statistically significant (Table G.1). On The Pile, Figure H.1 and Table H.1 similarly show that $d \propto D$, where the linear relationship is highly significant; the high effect size $\alpha = 0.81$, in this case, indicates that the model tends to fill the ambient space such that $d \approx D$. While for The Pile, $I_d \propto D$ ($R = 0.95$, $p < 0.001$) as well, the tiny effect size $\alpha = 0.002$ shows that I_d changes negligibly with respect to D , seen in Figure H.1 (left).

These results highlight key differences in how linear and nonlinear dimensions are recruited: LMs *globally* distribute representations to occupy $d \propto D$ dimensions of the space, but their shape is *locally* constrained to a low-dimensional (I_d) manifold. Robustness of I_d to scaling the hidden dimension suggests that LMs, once sufficiently performant, recover the degrees of freedom underlying the data.

4.2 EVOLUTION OF REPRESENTATIONAL GEOMETRY TRACKS EMERGENT LINGUISTIC ABILITIES OVER TRAINING

We just saw how dimensionality scales with size, and now we investigate its change over time. We find that feature complexity is highly related to the LM’s linguistic capabilities, assessed using the eval-harness benchmark performance, over training. Figure 3 shows the evolution of I_d on the $k = 1$ dataset (top), where each curve is one layer, with the evolution of LM performance on the benchmark tasks (bottom), where each curve plots performance on an individual task.

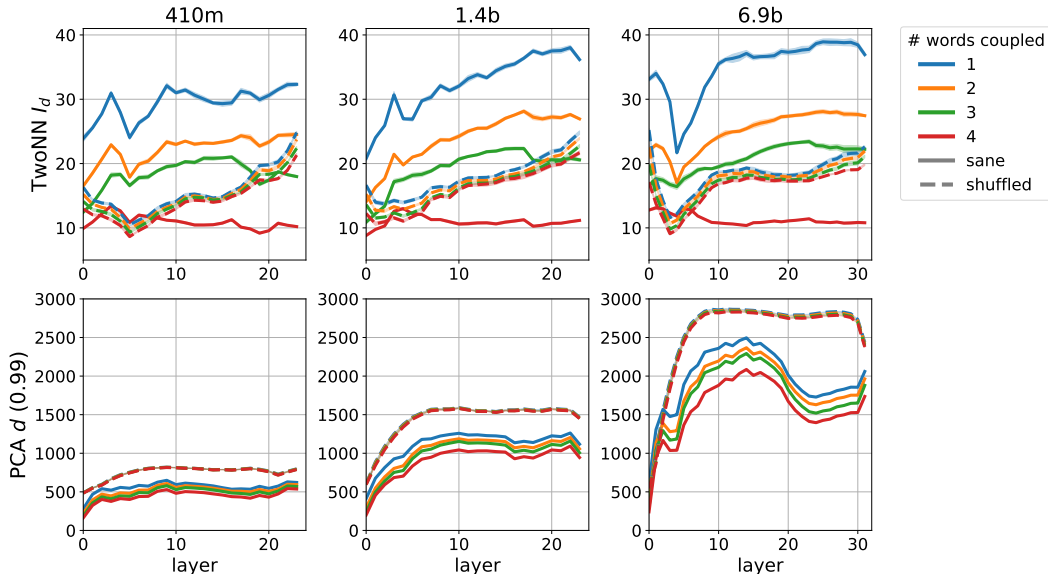


Figure 4: **Dimensionality over layers.** Nonlinear I_d (top) and linear d (bottom) over layers are shown for sizes 410m, 1.4b, and 6.9b (left to right). Each color corresponds to a coupling length $k \in 1 \dots 4$. Solid curves denote sane sequences, and dotted curves denote shuffled sequences. For all models, lower k results in higher I_d and d for both normal and shuffled settings. For all models, shuffling results in lower I_d but higher d . Curves are averaged over 5 random data splits, shown with ± 1 SD (shaded); SDs across random data splits tended to be very small.

We observe in Figure 3 that, for all models, the evolution of representational dimensionality closely tracks a sudden transition in LM task performance. In Figure 3 top, we first observe that I_d decreases sharply before checkpoint 10^3 and then re-distributes. At the same time, task performance rapidly improves after the steep decrease in I_d (Figure 3 bottom). Feature complexity evolution on The Pile is shown in Figure H.2, and exhibits a similar transition to that reported in Figure 3. Further, the existence of the phase transition in representational geometry $t \approx 10^3$ is robust to the dimensionality measure and whether the data are shuffled, see Figure G.4. Our results resonate with Chen et al. (2024), who observed in BERT models a similar two-part I_d transition on the training corpus; they showed that the two extrema corresponding to the dip and uptick in I_d temporally coincided with the onset of higher-order linguistic capabilities. Together, results show that representational complexity can signify whether and when LMs learn linguistic structure. Crucially, we show that the phase transition exists for inputs *beyond* in-distribution data, which was the subject of (Chen et al., 2024), and, furthermore, beyond grammatical data (Figure G.4) as a more general property of LM processing.

4.3 REPRESENTATIONAL COMPLEXITY REFLECTS INPUT COMPOSITIONALITY

We just established that feature complexity is informative of when models gain complex linguistic capabilities that, by definition, require compositional understanding. Now, we establish our key result, which is that **feature complexity encodes input compositionality**, both when considering formal compositionality, or data combinatorial complexity, as well as meaning compositionality, or sentence-level semantics. We first show that this holds for fully-trained models that have reached final linguistic competency. Then, using evidence from the training phase of the model, we show that the correspondence between feature complexity and input compositionality is present first as an inductive bias of the model that encodes formal complexity; but then, that it persists due to learned syntactic and semantic features that encode meaning complexity. Lastly, we further develop the coding differences between d and I_d , confirming an existing hypothesis in the literature (Recanatani et al., 2021) that they respectively encode formal and semantic complexity of inputs.

Data combinatorial complexity On fully-trained models, representational dimensionality preserves relative dataset compositionality. Figure 4 shows for fully-trained Pythia 410m, 1.4b, and 6.9b that I_d and d increase with the degree of formal compositionality within both sane (solid) and

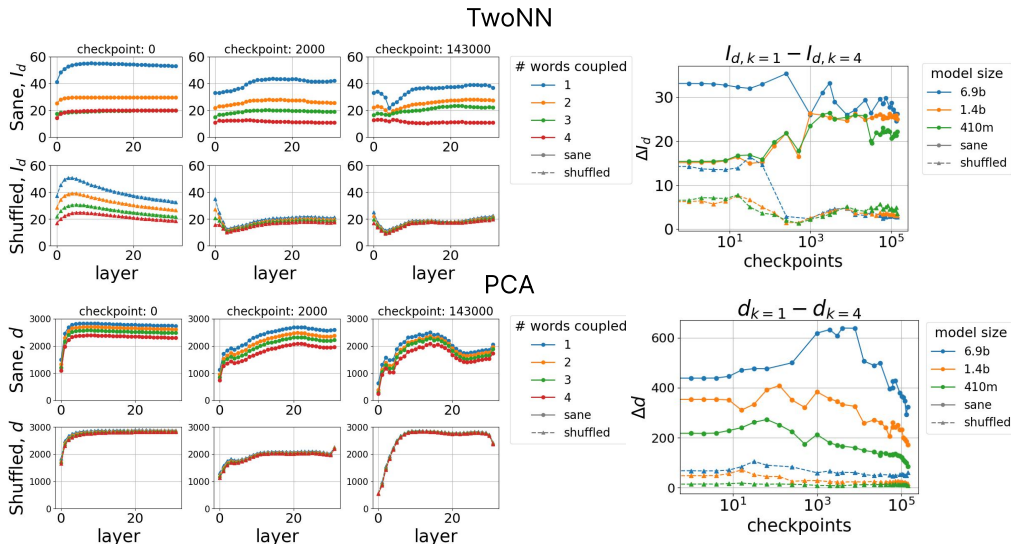


Figure 5: **Training dynamics of dimensionality.** The top row shows results for Twonn I_d and the bottom row shows the PCA d . **(Left):** Layerwise I_d at different timepoints of training for sane vs. shuffled examples with different coupling k (6.9b model). I_d difference of shuffled examples with varying k diminishes as the training persists. All curves are shown with ± 1 SD (the SDs were very small). **(Right):** ΔI_d between $k = 1, k = 4$ across training for various model sizes (different colors).

shuffled (dashed) settings: the highest curves (blue) correspond to the $k = 1$ dataset, or 12 degrees of freedom, and the lowest (red) denote the $k = 4$ dataset, or 3 degrees of freedom. The relative order of feature complexity, moreover, holds for all layers, seen by non-overlapping solid curves in Figure 4.

Grammaticality is not a precondition for representational dimensionality to reflect data combinatorial complexity: in Figure 4 (top), dashed curves corresponding to shuffled text are also ordered $k = 1 \dots 4$ top to bottom. While the relative order of formal complexity is preserved in the LM’s feature complexity for both grammatical and agrammatical datasets, the separation is greater for grammatical text (solid curves). We hypothesize that this is due to shuffled text being out-of-distribution, such that the model cannot integrate the sequences’ meaning, but nevertheless preserve surface-level complexity in its representations. This tendency holds for pre-trained models of all sizes, see Figure G.1.

The relationship between dimensionality and data combinatorial complexity, controlled by k , for sane text is *not* an emergent feature over training. In Figure 5 (left), the inverse relationship between k and both I_d and d is present throughout training. But, the reason for this relation differs at the start and end: in shuffled text, where sequence-level semantics are not present, the relationship between k and dimensionality is salient at the *beginning* and greatly diminishes by the end, whereas in sane text it remains salient throughout training. Together, these demonstrate an inductive bias of the initialized LM architecture to preserve input complexity in its representations. Then, over training, differences in dimensionality may be increasingly explained by features beyond the surface distribution of inputs. We claim that these features are semantic, providing evidence towards the claim in what follows.

Compositional semantics Shuffling sequences destroys their meaning, removing dataset complexity attributed to sentence-level semantics. Figure 4 shows, for fully-trained models, the dimensionality over layers for sane and shuffled inputs. Here, nonlinear and linear dimensionalities show opposing trends: I_d for shuffled text *collapses* to a low range, while d *increases*, seen by the dashed curves in each plot compared to solid curves. This tendency holds across model sizes, see Figure G.1.

We refer to the phenomenon in which shuffling destroys sequence-level semantics and I_d , also attested for sequences in Pythia’s training corpus (Cheng et al., 2024), as *shuffling feature collapse*. Evidence from the training dynamics of the LM further suggests that this feature collapse is due to semantics. We saw in Section 4.2 that training step $t = 10^3$ approximately marked a phase transition after which the LM’s linguistic competencies sharply rose. Crucially, the epoch $t = 10^3$ preceding the sharp

Table 1: **Spearman correlations between dimensionality and estimated Kolmogorov complexity.** The Spearman correlation ρ between the `gzip` dataset size (KB) and representational dimensionality (rows), averaged over layers, is shown for all tested model sizes (columns). Values marked with a * are significant with a p-value threshold of 0.05. Values marked with a † are significant with a p-value threshold of 0.1. Generally across models, average-layer I_d is not correlated to the estimated Kolmogorov complexity, or formal compositionality, of datasets. Average-layer linear d is consistently highly positively correlated to the estimated Kolmogorov complexity, except one outlier (160m).

Spearman ρ	14m	70m	160m	410m	1.4b	6.9b	12b
I_d	-0.20	-0.06	-0.20	-0.05	0.04	0.01	0.05
d	0.90*	0.47†	-0.50†	0.96*	0.96*	0.92*	0.86*

increase in linguistic capabilities is also the first to exhibit shuffling feature collapse. Figure 5 (right) shows the ΔI_d between the $k = 1$ and $k = 4$ dataset for several model sizes, across training (x-axis). Shuffling feature collapse, given by low ΔI_d , occurs around $t = 10^3$ for all models. On the other hand, ΔI_d for sane text stabilizes to around ~ 25 for different model sizes. This transition does not occur for linear d , see Figure 5 (right, bottom). This suggests that shuffling feature collapse for I_d is symptomatic of when the LM learns to extract meaningful semantic features.

We interpret shuffling feature collapse using an argument from Recanatesi et al. (2021), who propose that predictive coding requires the model to satisfy two objectives: to encode the vast “space of inputs and outputs”, exerting upward pressure on representational complexity, and at the same time, to extract latent features to support prediction, exerting a downward pressure on complexity. Recanatesi et al. (2021) suggest that the first pressure expands the linear representation space \mathbb{R}^d , while the second compresses representations to a I_d -dimensional manifold. Indeed, in our setting, shuffling words increases input complexity, thus increasing d . But, shuffling destroys sequence semantics, exerting a downward pressure on I_d . Recanatesi et al. (2021)’s interpretation of linear dimensions as encoding the input space corresponds to what we have been calling *formal compositionality*; conversely, what they refer to as latent semantic features, encoded nonlinearly, is aligned with our *meaning compositionality*. We now investigate this form-meaning coding dichotomy in more detail.

Form-meaning dichotomy in representation learning We proposed in line with Recanatesi et al. (2021) that linear d captures surface-level variation, while I_d primarily encodes semantic variation. We have shown the latter in the previous section: I_d decreases in the absence of compositional semantics while d does not, suggesting that I_d , not d , encodes sequence-level meaning complexity. If this hypothesis holds, we need to show that linear d , and not I_d , encodes form compositionality.

Form compositionality is quantified by the `gzip`-compressed size of each dataset. Spearman correlations between `gzip` (kilobytes), and dimensionality are shown in Table 1. Consistently across model sizes, the average layerwise I_d is not correlated to `gzip` size, while the average layerwise d is highly correlated to `gzip` size; we discuss the outlier 160m in Appendix I. The high correlation between d and `gzip` size is, moreover, surprisingly consistent across layers, see Figure I.1, and already present as an inductive bias of the initialized model (see Figure I.2, Appendix I for training dynamics discussion), while the correlation to I_d is highly variable and seldom significant for all of training. This suggests that form complexity, already present in the inputs to the LM, is superficially *preserved*, while meaning complexity is instead *constructed*, over layers and over training.

5 DISCUSSION

We have studied language model compositionality from a geometric and dynamic perspective. Using a carefully curated synthetic dataset, we found strong relationships between the compositionality of linguistic expressions and the dimensionality of their representations. On one hand, representational dimensionality is positively correlated to datasets’ formal, or combinatorial, complexity. On the other hand, grammatical sequences, whose semantics are composed via syntax, tend to exhibit a higher non-linear dimensionality, but a lower linear dimensionality, than agrammatical shuffled sequences. We showed that the positive relationship between compositionality and dimensionality is an inductive

bias of the model, but that it is eventually shed in favor of learning a representation manifold that reflects meaningful *semantic* complexity in a phase transition. Results suggested differential coding of form and meaning in LM representations, where form complexity, estimated with `gzip`, is expressed linearly, and meaning complexity is expressed nonlinearly.

A central throughline in our results is that LMs compress representations to low-dimensional nonlinear manifolds, yet expand them to high-dimensional linear subspaces. This echoes independent results in computational neuroscience by Manley et al. (2024), who found that linear dimensionality scaled with number of neurons recorded in the mouse cortex, and De & Chaudhuri (2023), who found in neural networks that nonlinear, rather than linear, dimensionality better captured task semantics. The tendency for LMs to compress data to low-dimensional nonlinear manifolds, but, at the same time, expand them into high-dimensional linear subspaces, suggests a solution to the curse of dimensionality that also enjoys its blessings. High-dimensional representations classically engender overfitting and poor generalization (Hughes, 1968); but, these high-dimensional representations may lie on manifolds whose ID actually captures the latent sparsity of the data (De & Chaudhuri, 2023). At the same time, more dimensions implies more expressive orthogonality relations and linear decodability of categories (Cohen et al., 2020; Elmoznino & Bonner, 2023; Sorscher et al., 2022). Benefits of this dual patterning of intrinsic and effective dimensionality have been observed in biological and artificial intelligence (Jazayeri & Ostojic, 2021; Recanatesi et al., 2021; Haxby et al., 2011; Huth et al., 2012; De & Chaudhuri, 2023), where moreover, (linear) dimensional expansion and compression have implications for “lazy” and “rich” feature learning regimes, respectively (Flesch et al., 2022). While the present work is the first to show that this dual patterning in LMs broadly corresponds to a form-meaning dichotomy in representation learning, further work is needed to disentangle how nonlinear and linear features causally contribute to predictive coding.

REPRODUCIBILITY STATEMENT

In Section 3.1, we have outlined the language models used in our experiments. The synthetic and naturalistic datasets employed to study compositionality and geometric feature complexity are introduced in Section 3.2 and further detailed in Appendix E. A comprehensive description of the measures used to assess representation geometric complexity is provided in Section 3.3, Appendix D, and Appendix C. Additionally, the benchmark tasks used to evaluate the Pythia checkpoints are summarized in Appendix F. Computing resources are described in Appendix A, and links to the assets used and their licenses are provided in Appendix B.

ACKNOWLEDGEMENTS

This project has received funding from the European Research Council (ERC) under the European Union’s Horizon 2020 research and innovation programme (grant agreement No. 101019291). This paper reflects the authors’ view only, and the funding agency is not responsible for any use that may be made of the information it contains. JHL thanks the Gatsby Charitable Foundation (GAT3755) and The Wellcome Trust (219627/Z/19/Z). TJ is funded by FRQNT. EC, JHL and TJ thank the Center for Brain, Minds and Machines for hosting the collaboration.

The authors thank Marco Baroni, Noga Zaslavsky, Erin Grant, Francesca Franzon, Alessandro Laio, Andrew Saxe, and members of the COLT group at Universitat Pompeu Fabra for valuable feedback.

AUTHOR CONTRIBUTIONS

EC and LY contributed the idea of exploring ID, compression, and linguistic compositionality in the static setting. JHL greatly expanded this idea to incorporate investigation of dynamics and evolution of the features of interest over training. EC, JHL and TJ created the grammar, implemented and ran experiments; TJ led the static, and JHL led the dynamic, comparison of geometry to compositionality. EC helped with computation, did Kolmogorov complexity experiments with TJ, and led the writing. All authors heavily contributed to the manuscript.

REFERENCES

- Emmanuel Abbe, Samy Bengio, Enric Boix-Adserà, Etai Littwin, and Joshua M. Susskind. Transformers learn through gradual rank increase. In *Thirty-seventh Conference on Neural Information Processing Systems, 2023*. URL <https://openreview.net/forum?id=qieeNl03C7>.
- Armen Aghajanyan, Sonal Gupta, and Luke Zettlemoyer. Intrinsic dimensionality explains the effectiveness of language model fine-tuning. In *Proceedings of the 59th Annual Meeting of the Association for Computational Linguistics and the 11th International Joint Conference on Natural Language Processing (Volume 1: Long Papers)*, pp. 7319–7328, Online, August 2021. Association for Computational Linguistics.
- Luca Albergante, Jonathan Bac, and Andrei Zinovyev. Estimating the effective dimension of large biological datasets using fisher separability analysis. In *2019 International Joint Conference on Neural Networks (IJCNN)*, pp. 1–8, Jul 2019. doi: 10.1109/IJCNN.2019.8852450.
- Matteo Alleman, Jonathan Mamou, Miguel A Del Rio, Hanlin Tang, Yoon Kim, and SueYeon Chung. Syntactic perturbations reveal representational correlates of hierarchical phrase structure in pretrained language models. In Anna Rogers, Iacer Calixto, Ivan Vulić, Naomi Saphra, Nora Kassner, Oana-Maria Camburu, Trapit Bansal, and Vered Shwartz (eds.), *Proceedings of the 6th Workshop on Representation Learning for NLP (Repl4NLP-2021)*, pp. 263–276, Online, August 2021. Association for Computational Linguistics. doi: 10.18653/v1/2021.repl4nlp-1.27. URL <https://aclanthology.org/2021.repl4nlp-1.27>.
- Jacob Andreas. Measuring compositionality in representation learning. *ArXiv*, abs/1902.07181, 2019. URL <https://api.semanticscholar.org/CorpusID:67749672>.
- Alessio Ansuini, Alessandro Laio, Jakob H Macke, and Davide Zoccolan. Intrinsic dimension of data representations in deep neural networks. In *Advances in Neural Information Processing Systems*, volume 32. Curran Associates, Inc., 2019.

- Dzmitry Bahdanau, Shikhar Murty, Michael Noukhovitch, Thien Huu Nguyen, Harm de Vries, and Aaron Courville. Systematic generalization: what is required and can it be learned? *arXiv preprint arXiv:1811.12889*, 2018.
- Randall Balestriero, Romain Cosentino, and Sarath Shekkizhar. Characterizing large language model geometry helps solve toxicity detection and generation. In *Forty-first International Conference on Machine Learning*, 2024. URL <https://openreview.net/forum?id=glfcwSsks8>.
- Marco Baroni. Linguistic generalization and compositionality in modern artificial neural networks. *Philosophical Transactions of the Royal Society B*, 375, 2019. URL <https://api.semanticscholar.org/CorpusID:90260325>.
- Luisa Bentivogli, Arianna Bisazza, Mauro Cettolo, and Marcello Federico. Neural versus phrase-based machine translation quality: a case study. In *Proceedings of the Conference on Empirical Methods in Natural Language Processing (EMNLP)*. Association for Computational Linguistics (ACL), 2016.
- Stella Biderman, Hailey Schoelkopf, Quentin Gregory Anthony, Herbie Bradley, Kyle O’Brien, Eric Hallahan, Mohammad Aflah Khan, Shivanshu Purohit, USVSN Sai Prashanth, Edward Raff, et al. Pythia: A suite for analyzing large language models across training and scaling. In *International Conference on Machine Learning*, pp. 2397–2430. PMLR, 2023.
- Yonatan Bisk, Rowan Zellers, Ronan Le Bras, Jianfeng Gao, and Yejin Choi. Piqa: Reasoning about physical commonsense in natural language, 2019. URL <https://arxiv.org/abs/1911.11641>.
- Yonatan Bisk, Rowan Zellers, Jianfeng Gao, Yejin Choi, et al. Piqa: Reasoning about physical commonsense in natural language. In *Proceedings of the AAAI conference on artificial intelligence*, volume 34, pp. 7432–7439, 2020.
- Xingyu Cai, Jiaji Huang, Yuchen Bian, and Kenneth Church. Isotropy in the contextual embedding space: Clusters and manifolds. In *International Conference on Learning Representations*, 2021.
- P. Campadelli, E. Casiraghi, C. Ceruti, and A. Rozza. Intrinsic dimension estimation: Relevant techniques and a benchmark framework. *Mathematical Problems in Engineering*, 2015:e759567, Oct 2015. ISSN 1024-123X.
- Angelica Chen, Ravid Shwartz-Ziv, Kyunghyun Cho, Matthew L Leavitt, and Naomi Saphra. Sudden drops in the loss: Syntax acquisition, phase transitions, and simplicity bias in MLMs. In *The Twelfth International Conference on Learning Representations*, 2024. URL <https://openreview.net/forum?id=MO5PiKHELW>.
- Emily Cheng, Corentin Kervadec, and Marco Baroni. Bridging information-theoretic and geometric compression in language models. In *Proceedings of EMNLP*, pp. 12397–12420, Singapore, 2023.
- Emily Cheng, Diego Doimo, Corentin Kervadec, Iuri Macocco, Jade Yu, Alessandro Laio, and Marco Baroni. Emergence of a high-dimensional abstraction phase in language transformers, 2024. URL <https://arxiv.org/abs/2405.15471>.
- Emmanuele Chersoni, Philippe Blache, and Alessandro Lenci. Towards a distributional model of semantic complexity. In Dominique Brunato, Felice Dell’Orletta, Giulia Venturi, Thomas François, and Philippe Blache (eds.), *Proceedings of the Workshop on Computational Linguistics for Linguistic Complexity (CLALC)*, pp. 12–22, Osaka, Japan, December 2016. The COLING 2016 Organizing Committee. URL <https://aclanthology.org/W16-4102>.
- Noam Chomsky. *Syntactic Structures*. Mouton and Co., The Hague, 1957.
- Noam Chomsky. Derivation by phase. 1999. URL <https://api.semanticscholar.org/CorpusID:118158028>.
- SueYeon Chung, Daniel D. Lee, and Haim Sompolinsky. Classification and geometry of general perceptual manifolds. *Phys. Rev. X*, 8:031003, Jul 2018.

- Peter Clark, Isaac Cowhey, Oren Etzioni, Tushar Khot, Ashish Sabharwal, Carissa Schoenick, and Oyvind Tafjord. Think you have solved question answering? try arc, the ai2 reasoning challenge. *arXiv preprint arXiv:1803.05457*, 2018.
- Uri Cohen, SueYeon Chung, Daniel D. Lee, and Haim Sompolinsky. Separability and geometry of object manifolds in deep neural networks. *Nature Communications*, 11(1):746, Feb 2020. ISSN 2041-1723. doi: 10.1038/s41467-020-14578-5. URL <https://www.nature.com/articles/s41467-020-14578-5>.
- Verna Dankers, Christopher Lucas, and Ivan Titov. Can transformer be too compositional? analysing idiom processing in neural machine translation. In Smaranda Muresan, Preslav Nakov, and Aline Villavicencio (eds.), *Proceedings of the 60th Annual Meeting of the Association for Computational Linguistics (Volume 1: Long Papers)*, pp. 3608–3626, Dublin, Ireland, May 2022. Association for Computational Linguistics. doi: 10.18653/v1/2022.acl-long.252. URL <https://aclanthology.org/2022.acl-long.252>.
- Anandita De and Rishidev Chaudhuri. Common population codes produce extremely nonlinear neural manifolds. *Proceedings of the National Academy of Sciences*, 120(39):e2305853120, 2023. doi: 10.1073/pnas.2305853120. URL <https://www.pnas.org/doi/abs/10.1073/pnas.2305853120>.
- Ferdinand de Saussure. *Cours de linguistique générale*. Payot, Paris, 1916.
- Robert Mw Dixon. Iwhere have all the adjectives gone. *Studies in Language*, 1:19–80, 1976.
- Diego Doimo, Alessandro Serra, Alessio Ansuini, and Alberto Cazzaniga. The representation landscape of few-shot learning and fine-tuning in large language models, 2024. URL <https://arxiv.org/abs/2409.03662>.
- Nelson Elhage, Neel Nanda, Catherine Olsson, Tom Henighan, Nicholas Joseph, Ben Mann, Amanda Askell, Yuntao Bai, Anna Chen, Tom Conerly, Nova DasSarma, Dawn Drain, Deep Ganguli, Zac Hatfield-Dodds, Danny Hernandez, Andy Jones, Jackson Kernion, Liane Lovitt, Kamal Ndousse, Dario Amodei, Tom Brown, Jack Clark, Jared Kaplan, Sam McCandlish, and Chris Olah. A mathematical framework for transformer circuits. *Transformer Circuits Thread*, 2021. <https://transformer-circuits.pub/2021/framework/index.html>.
- Eric Elmoznino and Michael F. Bonner. High-performing neural network models of visual cortex benefit from high latent dimensionality. *PLOS Computational Biology*, 20, 2023. URL <https://api.semanticscholar.org/CorpusID:250645686>.
- Joshua Engels, Isaac Liao, Eric J. Michaud, Wes Gurnee, and Max Tegmark. Not all language model features are linear, 2024. URL <https://arxiv.org/abs/2405.14860>.
- Elena Facco, Maria d’Errico, Alex Rodriguez, and Alessandro Laio. Estimating the intrinsic dimension of datasets by a minimal neighborhood information. *Scientific Reports*, 7(1):12140, Sep 2017. ISSN 2045-2322. doi: 10.1038/s41598-017-11873-y.
- Timo Flesch, Keno Juechems, Tsvetomira Dumbalska, Andrew Saxe, and Christopher Summerfield. Orthogonal representations for robust context-dependent task performance in brains and neural networks. *Neuron*, 110(7):1258–1270.e11, April 2022. ISSN 1097-4199. doi: 10.1016/j.neuron.2022.01.005.
- Jerry A Fodor and Zenon W Pylyshyn. Connectionism and cognitive architecture: A critical analysis. *Cognition*, 28(1-2):3–71, 1988.
- Gottlob Frege. Ueber sinn und bedeutung. *Philosophical Review*, 57(n/a):209, 1948.
- Leo Gao, Stella Biderman, Sid Black, Laurence Golding, Travis Hoppe, Charles Foster, Jason Phang, Horace He, Anish Thite, Noa Nabeshima, et al. The Pile: An 800GB dataset of diverse text for language modeling. *arXiv preprint arXiv:2101.00027*, 2020.

- Leo Gao, Jonathan Tow, Baber Abbasi, Stella Biderman, Sid Black, Anthony DiPofi, Charles Foster, Laurence Golding, Jeffrey Hsu, Alain Le Noac’h, Haonan Li, Kyle McDonell, Niklas Muennighoff, Chris Ociepa, Jason Phang, Laria Reynolds, Hailey Schoelkopf, Aviya Skowron, Lintang Sutawika, Eric Tang, Anish Thite, Ben Wang, Kevin Wang, and Andy Zou. A framework for few-shot language model evaluation, 07 2024. URL <https://zenodo.org/records/12608602>.
- Peiran Gao, Eric M. Trautmann, Byron M. Yu, Gopal Santhanam, Stephen I. Ryu, Krishna V. Shenoy, and Surya Ganguli. A theory of multineuronal dimensionality, dynamics and measurement. *bioRxiv*, 2017. URL <https://api.semanticscholar.org/CorpusID:19938440>.
- Mor Geva, Jasmijn Bastings, Katja Filippova, and Amir Globerson. Dissecting recall of factual associations in auto-regressive language models. In *Proceedings of the 2023 Conference on Empirical Methods in Natural Language Processing*, pp. 12216–12235, 2023.
- Ian Goodfellow, Yoshua Bengio, and Aaron Courville. *Deep Learning*. MIT Press, 2016. <http://www.deeplearningbook.org>.
- Adi Haviv, Ido Cohen, Jacob Gidron, Roei Schuster, Yoav Goldberg, and Mor Geva. Understanding transformer memorization recall through idioms. In *Proceedings of the 17th Conference of the European Chapter of the Association for Computational Linguistics*, pp. 248–264, 2023.
- James V. Haxby, J. Swaroop Guntupalli, Andrew C. Connolly, Yaroslav O. Halchenko, Bryan R. Conroy, Maria Ida Gobbi, Michael Hanke, and Peter J. Ramadge. A common, high-dimensional model of the representational space in human ventral temporal cortex. *Neuron*, 72:404–416, 2011. URL <https://api.semanticscholar.org/CorpusID:5051787>.
- Evan Hernandez and Jacob Andreas. The low-dimensional linear geometry of contextualized word representations. In *Proceedings of the 25th Conference on Computational Natural Language Learning*, pp. 82–93, Online, November 2021. Association for Computational Linguistics. doi: 10.18653/v1/2021.conll-1.7. URL <https://aclanthology.org/2021.conll-1.7>.
- G. Hughes. On the mean accuracy of statistical pattern recognizers. *IEEE Transactions on Information Theory*, 14(1):55–63, 1968. doi: 10.1109/TIT.1968.1054102.
- Dieuwke Hupkes, Verna Dankers, Mathijs Mul, and Elia Bruni. Compositionality decomposed: How do neural networks generalise? *J. Artif. Intell. Res.*, 67:757–795, 2019. URL <https://api.semanticscholar.org/CorpusID:211259383>.
- Alexander G. Huth, Shinji Nishimoto, An T. Vu, and Jack L. Gallant. A continuous semantic space describes the representation of thousands of object and action categories across the human brain. *Neuron*, 76:1210–1224, 2012. URL <https://api.semanticscholar.org/CorpusID:8271268>.
- Mehrdad Jazayeri and Srdjan Ostojic. Interpreting neural computations by examining intrinsic and embedding dimensionality of neural activity. *Current Opinion in Neurobiology*, 70:113–120, 2021. ISSN 0959-4388. doi: <https://doi.org/10.1016/j.conb.2021.08.002>. URL <https://www.sciencedirect.com/science/article/pii/S0959438821000933>. Computational Neuroscience.
- Zhiying Jiang, Matthew Yang, Mikhail Tsirlin, Raphael Tang, Yiqin Dai, and Jimmy Lin. “low-resource” text classification: A parameter-free classification method with compressors. In Anna Rogers, Jordan Boyd-Graber, and Naoaki Okazaki (eds.), *Findings of the Association for Computational Linguistics: ACL 2023*, pp. 6810–6828, Toronto, Canada, July 2023. Association for Computational Linguistics. doi: 10.18653/v1/2023.findings-acl.426. URL <https://aclanthology.org/2023.findings-acl.426>.
- Ian Jolliffe. *Principal Component Analysis*. Springer, 1986.
- Brenden Lake and Marco Baroni. Generalization without systematicity: On the compositional skills of sequence-to-sequence recurrent networks. In *International conference on machine learning*, pp. 2873–2882. PMLR, 2018.

- Hector Levesque, Ernest Davis, and Leora Morgenstern. The winograd schema challenge. In *Thirteenth international conference on the principles of knowledge representation and reasoning*, 2012.
- Elizaveta Levina and Peter Bickel. Maximum likelihood estimation of intrinsic dimension. In *Advances in Neural Information Processing Systems*, volume 17. MIT Press, 2004. URL https://papers.nips.cc/paper_files/paper/2004/hash/74934548253bcab8490ebd74afed7031-Abstract.html.
- Chunyuan Li, Heerad Farkhoor, Rosanne Liu, and Jason Yosinski. Measuring the intrinsic dimension of objective landscapes. In *International Conference on Learning Representations*, 2018.
- Jian Liu, Leyang Cui, Hanmeng Liu, Dandan Huang, Yile Wang, and Yue Zhang. Logiqa: A challenge dataset for machine reading comprehension with logical reasoning. *arXiv preprint arXiv:2007.08124*, 2020.
- Ekdeep Singh Lubana, Kyogo Kawaguchi, Robert P Dick, and Hidenori Tanaka. A percolation model of emergence: Analyzing transformers trained on a formal language. *arXiv preprint arXiv:2408.12578*, 2024.
- Anemily Machina and Robert Mercer. Anisotropy is not inherent to transformers. In Kevin Duh, Helena Gomez, and Steven Bethard (eds.), *Proceedings of the 2024 Conference of the North American Chapter of the Association for Computational Linguistics: Human Language Technologies (Volume 1: Long Papers)*, pp. 4892–4907, Mexico City, Mexico, June 2024. Association for Computational Linguistics. doi: 10.18653/v1/2024.naacl-long.274. URL <https://aclanthology.org/2024.naacl-long.274>.
- Jonathan Mamou, Hang Le, Miguel Del Rio, Cory Stephenson, Hanlin Tang, Yoon Kim, and Sueyeon Chung. Emergence of separable manifolds in deep language representations. In *Proceedings of the 37th International Conference on Machine Learning*, pp. 6713–6723. PMLR, Nov 2020. URL <https://proceedings.mlr.press/v119/mamou20a.html>.
- Jason Manley, Sihao Lu, Kevin Barber, Jeff Demas, Hyewon Kim, David Meyer, Francisca Martínez Traub, and Alipasha Vaziri. Simultaneous, cortex-wide dynamics of up to 1 million neurons reveal unbounded scaling of dimensionality with neuron number. *Neuron*, 112:1694–1709.e5, 2024. URL <https://api.semanticscholar.org/CorpusID:268253837>.
- Gary F Marcus. *The algebraic mind: Integrating connectionism and cognitive science*. MIT press, 2003.
- Richard Thomas McCoy. *IMPLICIT COMPOSITIONAL STRUCTURE IN THE VECTOR REPRESENTATIONS OF ARTIFICIAL NEURAL NETWORKS*. PhD thesis, Johns Hopkins University, July 2022. URL <http://jhir.library.jhu.edu/handle/1774.2/67617>.
- Shikhar Murty, Pratyusha Sharma, Jacob Andreas, and Christopher D Manning. Characterizing intrinsic compositionality in transformers with tree projections. In *The Eleventh International Conference on Learning Representations*.
- Denis Paperno, Germán Kruszewski, Angeliki Lazaridou, Quan Ngoc Pham, Raffaella Bernardi, Sandro Pezzelle, Marco Baroni, Gemma Boleda, and Raquel Fernández. The lambda dataset: Word prediction requiring a broad discourse context. *arXiv preprint arXiv:1606.06031*, 2016.
- Kiho Park, Yo Joong Choe, Yibo Jiang, and Victor Veitch. The geometry of categorical and hierarchical concepts in large language models. *ArXiv*, abs/2406.01506, 2024. URL <https://api.semanticscholar.org/CorpusID:270216615>.
- Shannon Pollard and Alan W. Biermann. A measure of semantic complexity for natural language systems. In *NAACL-ANLP 2000 Workshop on Syntactic and semantic complexity in natural language processing systems -*, volume 1, pp. 42–46, Seattle, Washington, 2000. Association for Computational Linguistics. doi: 10.3115/1117543.1117550. URL <http://portal.acm.org/citation.cfm?doid=1117543.1117550>.

- Phil Pope, Chen Zhu, Ahmed Abdelkader, Micah Goldblum, and Tom Goldstein. The intrinsic dimension of images and its impact on learning. In *International Conference on Learning Representations*, 2021.
- Ofir Press, Muru Zhang, Sewon Min, Ludwig Schmidt, Noah Smith, and Mike Lewis. Measuring and narrowing the compositionality gap in language models. In Houda Bouamor, Juan Pino, and Kalika Bali (eds.), *Findings of the Association for Computational Linguistics: EMNLP 2023*, pp. 5687–5711, Singapore, December 2023. Association for Computational Linguistics. doi: 10.18653/v1/2023.findings-emnlp.378. URL <https://aclanthology.org/2023.findings-emnlp.378>.
- Michael Psenka, Druv Pai, Vishal Raman, Shankar Sastry, and Yi Ma. Representation learning via manifold flattening and reconstruction. *Journal of Machine Learning Research*, 25(132):1–47, 2024.
- Giovanni Puccetti, Anna Rogers, Aleksandr Drozd, and Felice Dell’Orletta. Outlier dimensions that disrupt transformers are driven by frequency. In Yoav Goldberg, Zornitsa Kozareva, and Yue Zhang (eds.), *Findings of the Association for Computational Linguistics: EMNLP 2022*, pp. 1286–1304, Abu Dhabi, United Arab Emirates, December 2022. Association for Computational Linguistics. doi: 10.18653/v1/2022.findings-emnlp.93. URL <https://aclanthology.org/2022.findings-emnlp.93>.
- Stefano Recanatesi, Matthew Farrell, Madhu Advani, Timothy Moore, Guillaume Lajoie, and Eric Shea-Brown. Dimensionality compression and expansion in deep neural networks. Oct 2019. doi: 10.48550/arXiv.1906.00443. URL <http://arxiv.org/abs/1906.00443>. arXiv:1906.00443 [cs, stat].
- Stefano Recanatesi, Matthew Farrell, Guillaume Lajoie, Sophie Deneve, Mattia Rigotti, and Eric Shea-Brown. Predictive learning as a network mechanism for extracting low-dimensional latent space representations. *Nature Communications*, 12(1):1417, March 2021. ISSN 2041-1723. doi: 10.1038/s41467-021-21696-1.
- William Rudman, Catherine Chen, and Carsten Eickhoff. Outlier dimensions encode task specific knowledge. In Houda Bouamor, Juan Pino, and Kalika Bali (eds.), *Proceedings of the 2023 Conference on Empirical Methods in Natural Language Processing*, pp. 14596–14605, Singapore, December 2023. Association for Computational Linguistics. doi: 10.18653/v1/2023.emnlp-main.901. URL <https://aclanthology.org/2023.emnlp-main.901>.
- Keisuke Sakaguchi, Ronan Le Bras, Chandra Bhagavatula, and Yejin Choi. Winogrande: An adversarial winograd schema challenge at scale. *Communications of the ACM*, 64(9):99–106, 2021.
- Aalok Sathe, Evelina Fedorenko, and Noga Zaslavsky. Language use is only sparsely compositional: The case of english adjective-noun phrases in humans and large language models. In *Proceedings of the Annual Meeting of the Cognitive Science Society*, volume 46, 2023.
- Aaditya Singh, Stephanie Chan, Ted Moskovitz, Erin Grant, Andrew Saxe, and Felix Hill. The transient nature of emergent in-context learning in transformers. *Advances in Neural Information Processing Systems*, 36, 2024.
- Paul Smolensky. Tensor product variable binding and the representation of symbolic structures in connectionist systems. *Artificial intelligence*, 46(1-2):159–216, 1990.
- Ben Sorscher, Surya Ganguli, and Haim Sompolinsky. Neural representational geometry underlies few-shot concept learning. *Proceedings of the National Academy of Sciences*, 119(43): e2200800119, October 2022. doi: 10.1073/pnas.2200800119.
- Curt Tigges, Michael Hanna, Qinan Yu, and Stella Biderman. Llm circuit analyses are consistent across training and scale. *arXiv preprint arXiv:2407.10827*, 2024.
- William Timkey and Marten van Schijndel. All bark and no bite: Rogue dimensions in transformer language models obscure representational quality. In Marie-Francine Moens, Xuanjing Huang, Lucia Specia, and Scott Wen-tau Yih (eds.), *Proceedings of the 2021 Conference on Empirical*

Methods in Natural Language Processing, pp. 4527–4546, Online and Punta Cana, Dominican Republic, November 2021. Association for Computational Linguistics. doi: 10.18653/v1/2021.emnlp-main.372. URL <https://aclanthology.org/2021.emnlp-main.372>.

Eduard Tulchinskii, Kristian Kuznetsov, Kushnareva Laida, Daniil Cherniavskii, Sergey Nikolenko, Evgeny Burnaev, Serguei Barannikov, and Irina Piontkovskaya. Intrinsic dimension estimation for robust detection of AI-generated texts. In *Thirty-seventh Conference on Neural Information Processing Systems*, 2023. URL <https://openreview.net/forum?id=8uOZ0kNji6>.

Lucrezia Valeriani, Diego Doimo, Francesca Cuturello, Alessandro Laio, Alessio Ansuini, and Alberto Cazzaniga. The geometry of hidden representations of large transformer models. (arXiv:2302.00294), Feb 2023. doi: 10.48550/arXiv.2302.00294. URL <http://arxiv.org/abs/2302.00294>. arXiv:2302.00294 [cs, stat].

Lucas Weber, Jaap Jumelet, Elia Bruni, and Dieuwke Hupkes. Interpretability of language models via task spaces. In Lun-Wei Ku, Andre Martins, and Vivek Srikumar (eds.), *Proceedings of the 62nd Annual Meeting of the Association for Computational Linguistics (Volume 1: Long Papers)*, pp. 4522–4538, Bangkok, Thailand, August 2024. Association for Computational Linguistics. URL <https://aclanthology.org/2024.acl-long.248>.

Jason Wei, Yi Tay, Rishi Bommasani, Colin Raffel, Barret Zoph, Sebastian Borgeaud, Dani Yogatama, Maarten Bosma, Denny Zhou, Donald Metzler, Ed H. Chi, Tatsunori Hashimoto, Oriol Vinyals, Percy Liang, Jeff Dean, and William Fedus. Emergent abilities of large language models. *Transactions on Machine Learning Research*, 2022. ISSN 2835-8856. URL <https://openreview.net/forum?id=yzkSU5zdwD>. Survey Certification.

Johannes Welbl, Nelson F Liu, and Matt Gardner. Crowdsourcing multiple choice science questions. *arXiv preprint arXiv:1707.06209*, 2017.

Zhong Zhang, Bang Liu, and Junming Shao. Fine-tuning happens in tiny subspaces: Exploring intrinsic task-specific subspaces of pre-trained language models. In *Proceedings of the 61st Annual Meeting of the Association for Computational Linguistics (Volume 1: Long Papers)*, pp. 1701–1713, Toronto, Canada, July 2023. Association for Computational Linguistics. doi: 10.18653/v1/2023.acl-long.95. URL <https://aclanthology.org/2023.acl-long.95>.

A COMPUTING RESOURCES

All experiments were run on a cluster with 12 nodes with 5 NVIDIA A30 GPUs and 48 CPUs each. Extracting LM representations took a few wall-clock hours per model-dataset computation. ID computation took approximately 0.5 hours per model-dataset computation. Taking parallelization into account, we estimate the overall wall-clock time taken by all experiments, including failed runs, preliminary experiments, etc., to be of about 10 days.

B ASSETS

Pile <https://huggingface.co/datasets/NeelNanda/pile-10k>; license: bigscience-bloom-rail-1.0

Pythia <https://huggingface.co/EleutherAI/pythia-6.9b-deduped>; license: apache-2.0

scikit-dimension <https://scikit-dimension.readthedocs.io/en/latest/>; license: bsd-3-clause

PyTorch <https://scikit-learn.org/>; license: bsd

C OTHER DIMENSIONALITY ESTIMATORS

Maximum Likelihood Estimator In addition to TwoNN, we considered Levina & Bickel (2004)’s Maximum Likelihood Estimator (MLE), a similar, nonlinear measure of I_d . MLE has been used in

prior works on representational geometry such as (Cai et al., 2021; Cheng et al., 2023; Pope et al., 2021), and similarly models the number of points in a neighborhood around a reference point x to follow a Poisson point process. For details we refer to the original paper (Levina & Bickel, 2004). Like past work (Facco et al., 2017; Cheng et al., 2023), we found MLE and TwoNN to be highly correlated, producing results that were nearly identical: compare Figure 2 left to Figure G.3 left, and Figure G.1 top to Figure G.2 top).

Participation Ratio For our primary linear measure of dimensionality d , we computed PCA and took the number of components that explain 99% of the variance. In addition to PCA, we computed the Participation Ratio (PR), defined as $(\sum_i \lambda_i)^2 / (\sum_i \lambda_i^2)$ (Gao et al., 2017). We found PR to give results that were incongruous with intuitions about linear dimensionality. In particular, it produced a lower dimensionality estimate than the nonlinear estimators we tested; see, e.g., Figure G.3, where the PR- d for sane text is less than that of TwoNN. This contradicts the mathematical relationship that $I_d \leq d \leq D$. This may be because, empirically, PR- d corresponded to explained variances of 60 – 80%, which are inadequate to describe the bounding linear subspace for the representation manifold. Therefore, while we report the mean PR- d over model size in Figure G.3 and the dimensionality over layers in Figure G.2 for completeness, we do not attempt to interpret them.

D INTRINSIC DIMENSION DETAILS

ID estimation methods practically rely on a finite set of points and their nearest-neighbor structure in order to compute an estimated dimensionality value. The underlying geometric calculations assume that these are points sampled from a continuum, such as a lower-dimensional non-linear manifold. In our case, we actually have a discrete set of points so the notion of an underlying manifold is not strictly applicable. However, we can ask the question: if those points had been sampled from a manifold, what would the estimated ID be? Since the algorithms themselves only require a discrete set of points, they can be used to answer that question.

E CONTROLLED GRAMMAR

The grammar is composed of sentences of the form

The [quality₁.ADJ][nationality₁.ADJ][job₁.N] [action₁.V] the [size₁.ADJ][texture.ADJ][color.ADJ][animal.N] then [action₂.V] the [size₂.ADJ][quality₂.ADJ][nationality₂.ADJ][job₂.N].

Each category, colored and enclosed in brackets, is sampled from a vocabulary of 50 possible words, listed in the table below:

Category	Words
job ₁	teacher, doctor, engineer, chef, lawyer, plumber, electrician, accountant, nurse, mechanic, architect, dentist, programmer, photographer, painter, firefighter, police, pilot, farmer, waiter, scientist, actor, musician, writer, athlete, designer, carpenter, librarian, journalist, psychologist, gardener, baker, butcher, tailor, cashier, barber, janitor, receptionist, salesperson, manager, tutor, coach, translator, veterinarian, pharmacist, therapist, driver, bartender, security, clerk

job ₂	banker, realtor, consultant, therapist, optometrist, astronomer, biologist, geologist, archaeologist, anthropologist, economist, sociologist, historian, philosopher, linguist, meteorologist, zoologist, botanist, chemist, physicist, mathematician, statistician, surveyor, pilot, steward, dispatcher, ichthyologist, oceanographer, ecologist, geneticist, microbiologist, neurologist, cardiologist, pediatrician, surgeon, anesthesiologist, radiologist, dermatologist, gynecologist, urologist, psychiatrist, physiotherapist, chiropractor, nutritionist, personal trainer, yoga instructor, masseur, acupuncturist, paramedic, midwife
animal	dog, cat, elephant, lion, tiger, giraffe, zebra, monkey, gorilla, chimpanzee, bear, wolf, fox, deer, moose, rabbit, squirrel, raccoon, beaver, otter, penguin, eagle, hawk, owl, parrot, flamingo, ostrich, peacock, swan, duck, frog, toad, snake, lizard, turtle, crocodile, alligator, shark, whale, dolphin, octopus, jellyfish, starfish, crab, lobster, butterfly, bee, ant, spider, scorpion
color	red, blue, green, yellow, purple, orange, pink, brown, gray, black, white, cyan, magenta, turquoise, indigo, violet, maroon, navy, olive, teal, lime, aqua, coral, crimson, fuchsia, gold, silver, bronze, beige, tan, khaki, lavender, plum, periwinkle, mauve, chartreuse, azure, mint, sage, ivory, salmon, peach, apricot, mustard, rust, burgundy, mahogany, chestnut, sienna, ochre
size ₁	big, small, large, tiny, huge, giant, massive, microscopic, enormous, colossal, miniature, petite, compact, spacious, vast, wide, narrow, slim, thick, thin, broad, expansive, extensive, substantial, boundless, considerable, immense, mammoth, towering, titanic, gargantuan, diminutive, minuscule, minute, hulking, bulky, hefty, voluminous, capacious, roomy, cramped, confined, restricted, limited, oversized, undersized, full, empty, half, partial
size ₂	lengthy, short, tall, long, deep, shallow, high, low, medium, average, moderate, middling, intermediate, standard, regular, normal, ordinary, sizable, generous, abundant, plentiful, copious, meager, scanty, skimpy, inadequate, sufficient, ample, excessive, extravagant, exorbitant, modest, humble, grand, majestic, imposing, commanding, dwarfed, diminished, reduced, enlarged, magnified, amplified, expanded, contracted, shrunken, swollen, bloated, inflated, deflated
nationality ₁	American, British, Canadian, Australian, German, French, Italian, Spanish, Japanese, Chinese, Indian, Russian, Brazilian, Mexican, Argentinian, Turkish, Egyptian, Nigerian, Kenyan, African, Swedish, Norwegian, Danish, Finnish, Icelandic, Dutch, Belgian, Swiss, Austrian, Greek, Polish, Hungarian, Czech, Slovak, Romanian, Bulgarian, Serbian, Croatian, Slovenian, Ukrainian, Belarusian, Estonian, Latvian, Lithuanian, Irish, Scottish, Welsh, Portuguese, Moroccan, Algerian
nationality ₂	Vietnamese, Thai, Malaysian, Indonesian, Filipino, Singaporean, Nepalese, Bangladeshi, Maldivian, Pakistani, Afghan, Iranian, Iraqi, Syrian, Lebanese, Israeli, Saudi, Emirati, Qatari, Kuwaiti, Omani, Yemeni, Jordanian, Palestinian, Bahraini, Tunisian, Libyan, Sudanese, Ethiopian, Somali, Ghanaian, Ivorian, Senegalese, Malian, Cameroonian, Congolese, Ugandan, Rwandan, Tanzanian, Mozambican, Zambian, Zimbabwean, Namibian, Botswanan, New Zealander, Fijian, Samoan, Tongan, Papuan, Marshallese

action ₁	feeds, walks, grooms, pets, trains, rides, tames, leashes, bathes, brushes, adopts, rescues, shelters, houses, cages, releases, frees, observes, studies, examines, photographs, films, sketches, paints, draws, catches, hunts, traps, chases, pursues, tracks, follows, herds, corrals, milks, shears, breeds, mates, clones, dissects, stuffs, mounts, taxidermies, domesticates, harnesses, saddles, muzzles, tags, chips, vaccinates
action ₂	hugs, kisses, loves, hates, admires, respects, befriends, distrusts, helps, hurts, teaches, learns from, mentors, guides, counsels, advises, supports, undermines, praises, criticizes, compliments, insults, congratulates, consoles, comforts, irritates, annoys, amuses, entertains, bores, inspires, motivates, discourages, intimidates, impresses, disappoints, surprises, shocks, delights, disgusts, forgives, resents, envies, pities, understands, misunderstands, trusts, mistrusts, betrays, protects
quality ₁	good, bad, excellent, poor, superior, inferior, outstanding, mediocre, exceptional, sublime, superb, terrible, wonderful, awful, great, horrible, fantastic, dreadful, marvelous, atrocious, splendid, appalling, brilliant, dismal, fabulous, lousy, terrific, abysmal, incredible, substandard, amazing, disappointing, extraordinary, stellar, remarkable, unremarkable, impressive, unimpressive, admirable, despicable, praiseworthy, blameworthy, commendable, reprehensible, exemplary, subpar, ideal, flawed, perfect, imperfect
quality ₂	acceptable, unacceptable, satisfactory, unsatisfactory, sophisticated, insufficient, adequate, exquisite, suitable, unsuitable, appropriate, inappropriate, fitting, unfitting, proper, improper, correct, incorrect, right, wrong, accurate, inaccurate, precise, imprecise, exact, inexact, flawless, faulty, sound, unsound, reliable, unreliable, dependable, undependable, trustworthy, untrustworthy, authentic, fake, genuine, counterfeit, legitimate, illegitimate, valid, invalid, legal, illegal, ethical, unethical, moral, immoral
texture	smooth, rough, soft, hard, silky, coarse, fluffy, fuzzy, furry, hairy, bumpy, lumpy, grainy, gritty, sandy, slimy, slippery, sticky, tacky, greasy, oily, waxy, velvety, leathery, rubbery, spongy, springy, elastic, pliable, flexible, rigid, stiff, brittle, crumbly, flaky, crispy, crunchy, chewy, stringy, fibrous, porous, dense, heavy, light, airy, feathery, downy, woolly, nubby, textured

F BENCHMARK TASKS

Here we briefly summarize the benchmark tasks that we use to evaluate Pythia checkpoints as described in Section 4.3. In figure 3, we did not include WSC (Winogrande Schema Challenge) which was originally included in Biderman et al., as it has been proposed that WSC dataset performance on LMs might be corrupted by spurious biases in the dataset (Sakaguchi et al., 2021). Instead, we only presented the evaluation from WinoGrande task, which is inspired from original WSC task but adjusted to reduce the systematic bias (Sakaguchi et al., 2021).

WinoGrande WinoGrande (Sakaguchi et al., 2021) is a dataset designed to test commonsense reasoning by building on the structure of the Winograd Schema Challenge (Levesque et al., 2012). It presents sentence pairs with subtle ambiguities where understanding the correct answer requires world knowledge and commonsense reasoning. It challenges models to differentiate between two possible resolutions of pronouns or references, making it a benchmark for evaluating an AI’s ability to understand context and reasoning.

LogiQA LogiQA (Liu et al., 2020) is an NLP benchmark for evaluating logical reasoning abilities in models. It consists of multiple-choice questions derived from logical reasoning exams for human students. The questions test various forms of logical reasoning, such as deduction, analogy, and quantitative reasoning, making it ideal for assessing how well AI can handle structured logical problems.

SciQ SciQ (Welbl et al., 2017) is a dataset focused on scientific question answering, based on material from science textbooks. It features multiple-choice questions related to science topics like biology, chemistry, and physics. The benchmark is designed to test a model’s ability to comprehend scientific information and answer questions using factual knowledge and reasoning.

ARC Challenge The ARC (AI2 Reasoning Challenge) Challenge Set (Clark et al., 2018) is a benchmark designed to test models on difficult, grade-school-level science questions. It presents multiple-choice questions that are challenging due to requiring complex reasoning, inference, and background knowledge beyond simple retrieval-based approaches. It is a tougher subset of the larger ARC dataset.

PIQA PIQA (Physical Interaction QA) (Bisk et al., 2020) is a benchmark designed to test models on physical commonsense reasoning. The questions require understanding basic physical interactions, like how objects interact or how everyday tasks are performed. It focuses on scenarios that involve intuitive knowledge of the physical world, making it a useful benchmark for evaluating practical commonsense in models.

ARC Easy ARC Easy is the easier subset of the AI2 Reasoning Challenge, consisting of grade-school-level science questions that require less complex reasoning compared to the Challenge set. This benchmark is meant to evaluate models’ ability to handle straightforward factual and retrieval-based questions, making it more accessible for baseline NLP models.

LAMBADA LAMBADA (Paperno et al., 2016) is a reading comprehension benchmark where models must predict the last word of a passage. The challenge lies in the fact that understanding the entire context of the passage is necessary to guess the correct word. This benchmark tests a model’s long-range context comprehension and coherence skills in natural language.

G ADDITIONAL RESULTS: CONTROLLED GRAMMAR

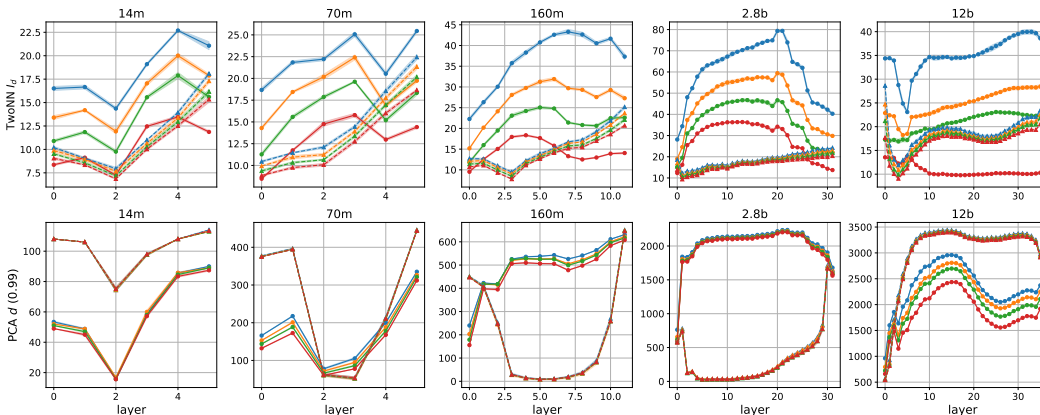


Figure G.1: **Dimensionality over layers.** TwoNN nonlinear I_d (top) and PCA linear d (bottom) over layers are shown for all sizes (left to right). Each color corresponds to a coupling length $k \in 1 \dots 4$. Solid curves denote sane sequences, and dotted curves denote shuffled sequences. For all models, lower k results in higher I_d and d for both normal and shuffled settings. For all models, shuffling results in lower I_d but higher d . Curves are averaged over 5 random seeds, shown with ± 1 SD.

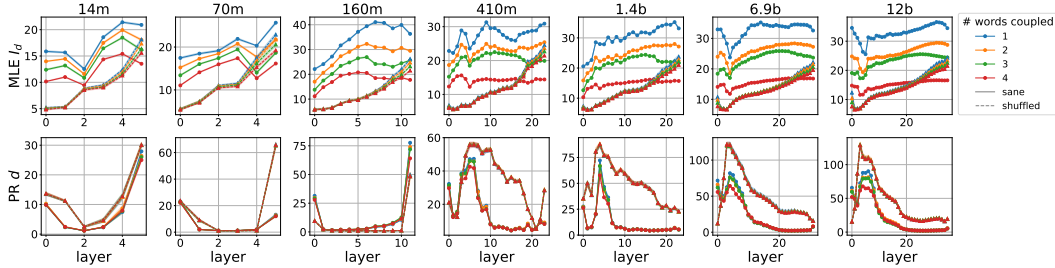


Figure G.2: **Other dimensionality metrics over layers.** MLE nonlinear I_d (top) and PR linear d (bottom) over layers are shown for all model sizes (left to right). Each color corresponds to a coupling length $k \in 1 \dots 4$. Solid curves denote sane sequences, and dotted curves denote shuffled sequences. For all models, lower k results in higher I_d for both normal and shuffled settings. For all models, shuffling results in lower I_d . The PR- d produced nonsensical results, with linear dimensionality higher than nonlinear dimensionality. Curves are averaged over 5 random seeds, shown with ± 1 SD.

Mode	k-coupling	PCA d			TwoNN I_d		
		α	R	p-value	α	R	p-value
sane	1	0.4598	0.9956	2×10^{-6}	0.0023	0.6341	0.1261
sane	2	0.4268	0.9954	3×10^{-6}	0.0011	0.5580	0.1930
sane	3	0.4014	0.9943	5×10^{-6}	0.0009	0.6616	0.1056
sane	4	0.3569	0.9924	1×10^{-5}	-0.0003	-0.3523	0.4383
shuffled	1	0.6239	0.9919	1.1×10^{-5}	0.0011	0.8488	0.0157
shuffled	2	0.6193	0.9917	1.2×10^{-5}	0.0010	0.8487	0.0157
shuffled	3	0.6153	0.9916	1.2×10^{-5}	0.0010	0.8586	0.0134
shuffled	4	0.6114	0.9916	1.2×10^{-5}	0.0009	0.8559	0.0140

Table G.1: **Linear regression of average layerwise dimensionality to hidden dimension, D .** For each setting (Mode, k -coupling columns) and dimensionality measure (PCA, TwoNN columns), the linear effect size α along with R -value and p -value are reported. PCA linear dimension shows a consistent strong linear relationship with large effect size α to hidden dimension D ($p < 0.001$) for all settings in $k = \{1 \dots 4\} \times [\text{sane}, \text{shuffled}]$. TwoNN intrinsic dimension does not scale linearly as D in all settings, showing a non-significant relationship for sane text and a significant one for shuffled text. For all TwoNN settings, the effect size α is near-zero, showing that nonlinear I_d is robust to changes in hidden dimension D .

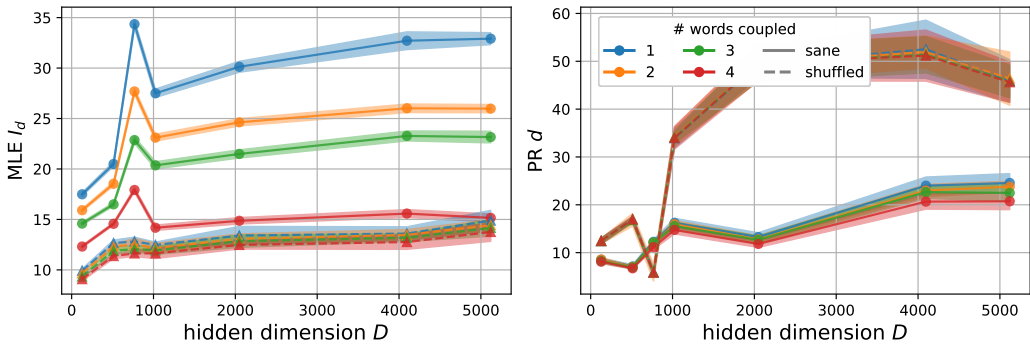


Figure G.3: **Mean dimensionality over model size (other metrics).** Mean nonlinear I_d computed with MLE (left) and linear d computed with PR (right) over layers is shown for increasing LM hidden dimension D . MLE I_d does not depend on extrinsic dimension D (flat lines). PR d produces nonsensical values, higher than the nonlinear I_d . Curves are averaged over 5 random seeds, shown with ± 1 SD.

H ADDITIONAL RESULTS: THE PILE

PCA d			TwoNN I_d		
α	R	p-value	α	R	p-value
0.8119	0.9993	2.39×10^{-8}	0.00173	0.9537	8.64×10^{-4}

Table H.1: **Linear regression of average layerwise dimensionality on The Pile to hidden dimension, D .** For dimensionality measures (PCA, TwoNN columns), the linear effect size α along with R -value and p -value are reported. PCA linear dimension shows a statistically significant linear relationship to D , with large effect size $\alpha = 0.81$. TwoNN intrinsic dimension also shows a slightly weaker, but still highly significant, linear relationship to D . But, the effect size α is near-zero, showing that nonlinear I_d is robust to changes in hidden dimension D .

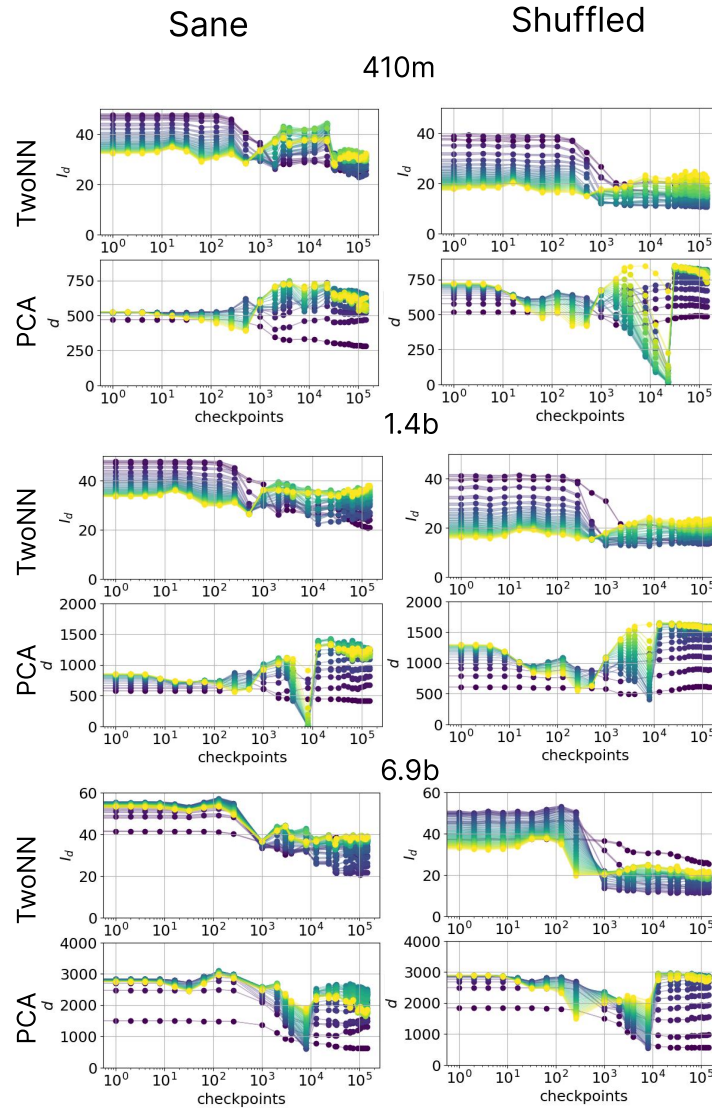


Figure G.4: **Layerwise feature complexity evolution over time, additional results.** Nonlinear I_d (top) and linear d (bottom) over training is shown for sane (left) and shuffled (right) text, for the 1-coupled setting. Each curve is one layer of the LM (yellow is later, purple is earlier). All settings in [TwoNN, PCA] \times [sane, shuffled] exhibit a phase transition in representational dimensionality at around checkpoint 10^3 , which corresponds to the sharp increase in task performance. In the nonlinear case (top row), the difference between layers' I_d is *low* at the end of training for shuffled text, and *high* for sane text. This suggests LM learns to perform meaningful and specialized processing over layers. The difference between layers' d (bottom row) at the end of training is, conversely, *high* for shuffled and *lower* for sane text. This is consistent with our interpretation of d as capturing implied dataset size.

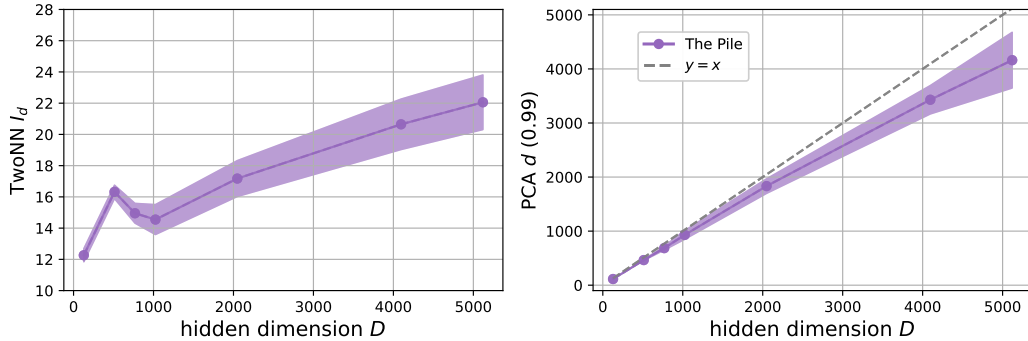


Figure H.1: **Mean dimensionality on the Pile over model size.** Mean nonlinear I_d computed with TwoNN (left) and linear d computed with PCA (right) over layers is shown for increasing LM hidden dimension D . TwoNN I_d grows very slowly with extrinsic dimension D , while PCA d grows to be nearly one-to-one with D . Curves are averaged over 5 random data splits, shown with ± 1 SD.

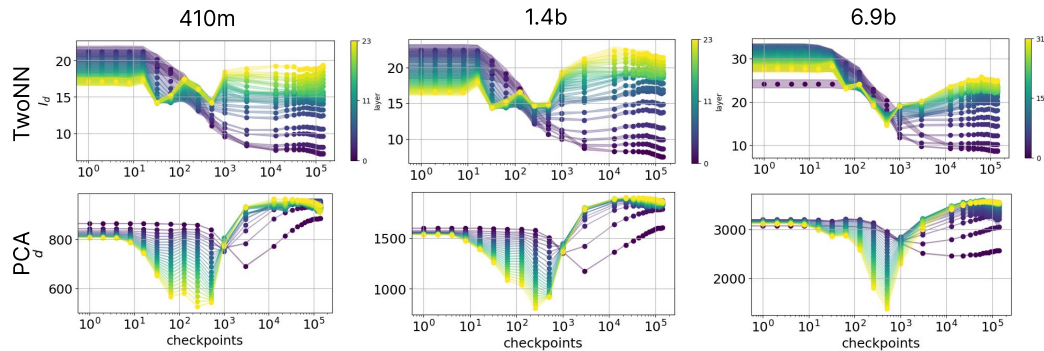


Figure H.2: **ID phase transition in The Pile.** Nonlinear I_d (top) and linear d (bottom) over training is shown for model sizes 410m, 1.4b, and 6.9b (left to right), for The Pile. Each curve is one layer of the LM (yellow is later, purple is earlier). Representations of The Pile exhibit a phase transition in both I_d and d at slightly before checkpoint 10^3 , where $t = 10^3$ corresponds to a dip and redistribution of layerwise dimensionality, and also a sharp increase in task performance in Figure 3.

I ADDITIONAL RESULTS: PER-LAYER CORRELATION WITH KOLMOGOROV COMPLEXITY

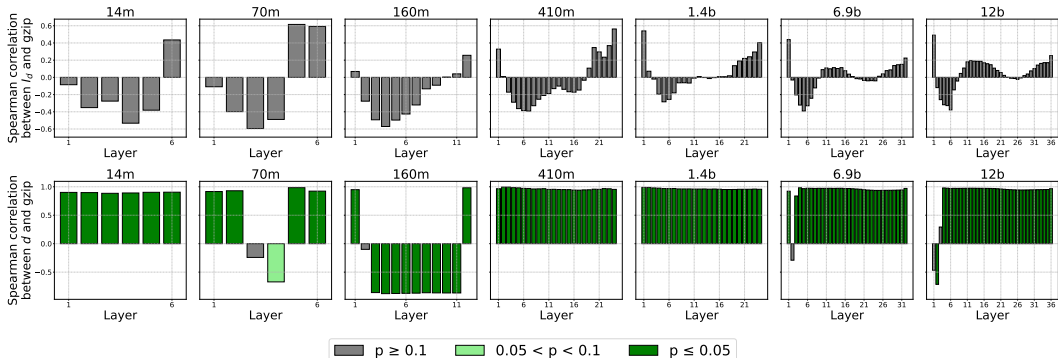


Figure I.1: **Spearman correlations between per-layer dimensionality and estimated Kolmogorov complexity.** The Spearman correlation between the gzipped dataset size (KB) and representational dimensionality per layer, is shown for all tested model sizes. Generally across models, per-layer I_d is not correlated to the estimated Kolmogorov complexity, or formal compositionality, of datasets. Per-layer linear d is consistently highly positively correlated to the estimated Kolmogorov complexity, except one outlier (160m).

Outliers There was one significant outlier, 160m, in our analysis correlating layerwise dimensionality to `gzip` (Kolmogorov complexity), see Figure I.1 and Table 1. While other models consistently demonstrate a positive Spearman correlation between d and `gzip` across layers, 160m (and to a smaller extent, 70m) deviates from this pattern. The reason 160m displays a negative correlation is due to its behavior on shuffled corpora, see the third column in Figure G.1: for intermediate layers, PCA with a variance threshold of 0.99 yields fewer than 50 PCs. We found that this was due to the existence of so-called “rogue dimensions” (Timkey & van Schijndel, 2021; Machina & Mercer, 2024; Rudman et al., 2023), where very few dimensions have outsized norms. Outlier dimensions have been found, via mechanistic interpretability analyses, to serve as a “sink” for uncertainty, and are associated to very frequent tokens in the training data (Puccetti et al., 2022). See Rudman et al. (2023) for exact activation profiles for the last-token embeddings in Pythia 70m and 160m. While increasing the variance threshold to 0.999 reduced the effect of rogue dimensions on PCA dimensionality estimation, we decided to keep the threshold at 0.99 for consistent comparison to other models.

Coding of formal complexity over training The Spearman correlations between layerwise dimensionality (I_d and d) and estimated Kolmogorov complexity using `gzip`, over training steps, are shown in Figure I.2 for 410m, 1.4b, and 6.9b. Each dot in the figure is a single layer’s correlation to `gzip`; each vertical set of dots is the distribution of correlations over layers, at a single timestep of training. Several observations stand out:

1. PCA encodes formal complexity (seen by earlier dots close to $\rho = 1.0$) as an inductive bias of the model architecture. The high correlation for most layers may be unlearned during intermediate checkpoints of model training, seen by the “dip” in gray dots around steps $10^2 \sim 10^3$, but is regained by the end of training for all model sizes. This indicates that encoding formal complexity at the end of training is a *learned behavior*.
2. TwoNN I_d does not statistically significantly correlate to `gzip` at any point during training, for virtually all layers.
3. For I_d , the phase transition noted in Section 4.2 is also present at slightly before $t = 10^3$; this is seen by layerwise correlations in Figure I.2a coalescing to around $\rho = 0.5$, and then redistributing. The layers that best encode formal complexity for TwoNN at the end of training correspond to model-initial and model-final layers, see Figure I.1 top.

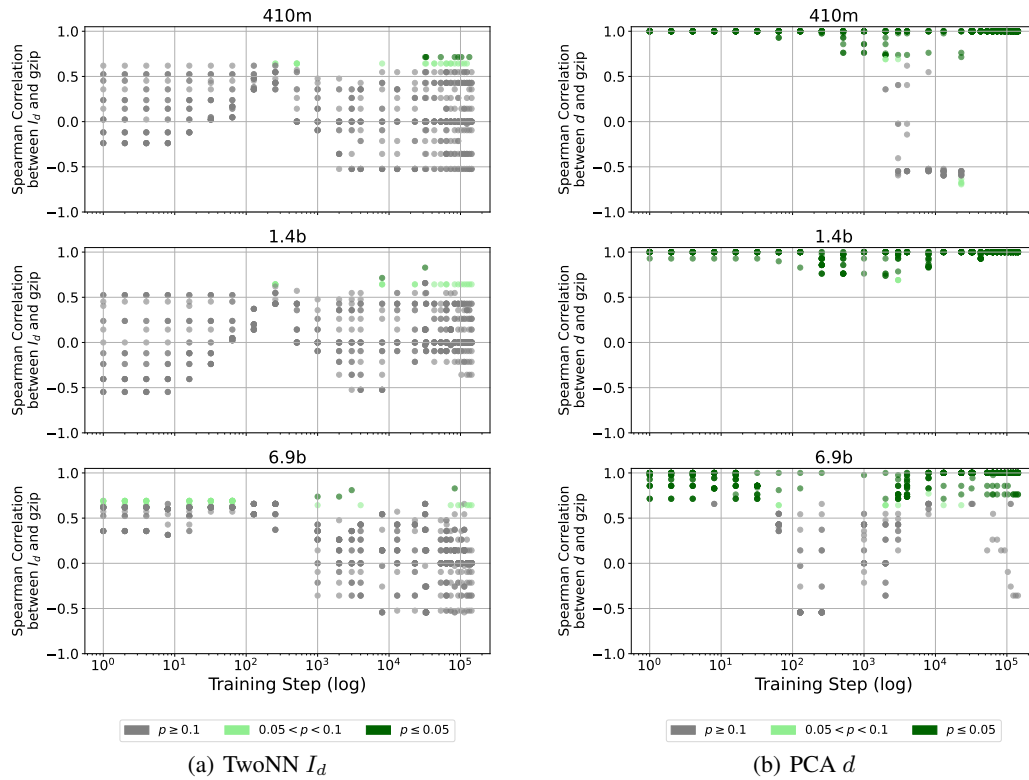


Figure I.2: **Spearman correlation of layerwise dimensionality and Kolmogorov complexity over training.** The Spearman correlations between I_d (left) and g_{zip} and d (right) and g_{zip} are plotted for three models, 410m, 1.4b, 6.9b (top to bottom) over training time (x axis), where correlation is computed across the controlled corpora. Each vertical set of points denotes the layer distribution of Spearman correlations at a single timestep; each point is one layer’s Spearman correlation, colored green if statistically significant and gray otherwise.